IEEE Access
The journal for rapid open access publishing

Received June 10, 2015, accepted June 26, 2015, date of publication July 8, 2015, date of current version July 29, 2015.

Digital Object Identifier 10.1109/ACCESS.2015.2453991

Ray Tracing for Radio Propagation Modeling: Principles and Applications

ZHENGQING YUN, (Member, IEEE), AND MAGDY F. ISKANDER, (Life Fellow, IEEE)
Hawaii Center for Advanced Communications, University of Hawaii at Manoa, Honolulu, HI 96822, USA

Corresponding author: Z. Yun (zyun@hawaii.edu)

This work was supported by the Division of Electrical, Communications and Cyber Systems through the U.S. National Science Foundation under Award 1443875 and by the U.S. Army Research Office under Award W911NF-14-1-057.

ABSTRACT This paper reviews the basic concepts of rays, ray tracing algorithms, and radio propagation modeling using ray tracing methods. We focus on the fundamental concepts and the development of practical ray tracing algorithms. The most recent progress and a future perspective of ray tracing are also discussed. We envision propagation modeling in the near future as an intelligent, accurate, and real-time system in which ray tracing plays an important role. This review is especially useful for experts who are developing new ray tracing algorithms to enhance modeling accuracy and improve computational speed.

INDEX TERMS Radio propagation, propagation modeling, ray tracing method, acceleration algorithm, GPU.

I. INTRODUCTION

The discovery of electromagnetic (EM) waves in 1880's by Hertz started a new era in scientific exploration of EM waves. In the application aspect, a major breakthrough occurred in 1901 when Marconi sent radio signals across the Atlantic Ocean: marking the beginning of the age of wireless communications [1]. During the last two decades or so, wireless/radio communication has undergone explosive development which, together with the Internet, played a key role in promoting globalization. There are 2.7 billion smart phone subscriptions in 2014 alone [2]. This number is expected to increase to 6.1 billion by 2020.

A key part of any wireless communications system is the wireless channel where the radio waves are employed to carry the signals or information. Although EM waves are governed by the Maxwell equations with appropriate boundary conditions, it is not possible in general to have an analytical solution for the EM field in a realistic propagation environment. The purpose of propagation modeling is to obtain an estimation of field/signal strengths when some of the parameters of the wireless system are given, such as the frequency, terrain characteristics, antenna heights, and so on.

The simplest propagation model is the Friis equation for free space radio propagation published in 1946 [3]. It relates the received power (P_r) to the transmitted power (P_t) as a function of the distance (r) between the two antennas (assuming matched impedance and polarization) and the wavelength (λ) of the EM waves; the effect of antenna gains, G_t and G_r, is also usually included:

$$\frac{P_r}{P_t} = G_t G_r \left(\frac{\lambda}{4\pi r}\right)^2 \tag{1}$$

The received power calculated using (1) is usually referred to as the direct field from a transmitting antenna. When there exist objects protruding into the first Fresnel zone defined by the transmitter (Tx) and receiver (Rx) locations, the free space assumption fails. The reflected and/or diffracted fields have to be calculated to count the effect of the objects. These effects are often related to the reflection from ground and diffraction from mountain peaks and ridges. For the reflection, the calculation is quite simple, but the diffracted field is much more difficult to determine.

Diffraction was investigated as early as the 1880's by Rayleigh and Kirchhoff for simple geometries and by others in the following decades (a good summary can be found in [4]). Diffraction from more realistic geometries were studied in 1940's. Most of the research aimed to obtain formulas for the calculation of diffractions due to *knife edges*.

Knife edge diffraction was an important research topic in the 1940's to 1980's. Several models have been developed and are widely used. In the Bullington model [5], [6], several obstacles are combined into one single knife edge and the diffraction loss is then calculated in a simpler manner. Other representative models are by Epstein and Peterson [7], Deygout (an improved version) [8], and others [9]. All these methods manipulate the geometry of the wedges and ray paths to obtain approximate results. These methods all rely on the height profile of the terrain and most of the three dimensional (3D) features of the terrain are ignored.

A comprehensive model for *irregular terrain* propagation prediction is the well-known Longley-Rice model which is still in use today. A detailed description of the model and its usage can be found in [10]. It requires a wide variety of input parameters from the wireless system (e.g., frequency, distance, antenna heights and polarization) and the environment (e.g., terrain irregularity, ground conductivity/permittivity, surface refractivity, and climate). It has been implemented in Fortran and C programming languages (about 1200 lines), downloadable from the Internet.

Empirical models are widely used and are developed based on extensive field measurements. One of the most famous empirical models is the Hata-Okumura model for urban regions [11]–[14]. The formula is expressed in dB units and is used to calculate the path loss L:

$$L = 10\log\left(\frac{P_t}{P_r}\right) = 69.55 + 26.16\log f_{MHz} - 13.82\log H_m - \alpha(h_m) + (44,9 - 6.55\log H_m)\log R_{km} \quad (2)$$

where f_{MHz} is the frequency in megahertz ($150\text{MHz} \le f_M \le 1500\text{MHz}$) and R_{km} is the distance in kilometers ($1\text{km} \le R_{km} \le 20\text{km}$). H_m and h_m are the heights of base station and mobile unit in meters ($30\text{m} \le H_m \le 200\text{m}$, $1\text{m} \le h_m \le 10\text{m}$). The $\alpha(h_m)$ term is a function of receive antenna height, frequency, and the size of the urban area. For more details, see [13], [14]. There exist extensions of the Hata-Okumura model, such as the COST-Hata-Model [15]. Other empirical models can be found in [13]–[16].

Theoretical models (e.g., the Friis model and the over-rooftop diffraction model) and empirical models are in general simple and fast in terms of computation. They also have satisfactory accuracy. The main drawbacks of empirical models include that they are in general, range-based and are valid only to the environment similar to the ones from which the models are developed. Also, for recently developed multiple-input multiple-output (MIMO) systems, empirical models are not able to provide accurate space-time or angle-delay results which are key characteristics for simulation of MIMO systems.

The ray tracing method, on the other hand, is based on the ray optics which solve the Maxwell's equations in high frequency regime. Thus, the ray tracing method is a general propagation modeling tool that provides estimates of path loss, angle of arrival/departure, and time delays. Unlike theoretical and empirical models, ray tracing method does not provide simple formulas for the calculation of path loss. It is a computer program and is a numerical method solving Maxwell's equations. Therefore, ray-tracing methods also belong to the computational EM (CEM) family where members such as the finite-difference time-domain (FDTD) method [17], the finite element method (FEM) [18], method of moments (MoM) [19], etc., are widely used in the design and simulation of EM systems.

It is well known that most CEM methods are computationally intensive. Due to the fact that a propagation environment is in most cases electrically large, numerical methods based on the discretization of differential or integral equations (FDTD, FEM, MoM) will face the challenges of prohibitively large memory needs and slow computational speed. Fortunately, the ray-tracing method, due to its high frequency approximation, is not so dependent on large computer memory. It has become a widely used CEM method in radio propagation modeling and it can solve 3D, electrically large problems on modern desktop computers. It should be pointed out that another numerical method, the parabolic equation method (PE), is able to tackle long range propagation problems. The PE method is an approximation method that seeks field solutions in a paraxial region [20]. This characteristics limits its application to long-range and narrow (angle) region above the earth's surface [21], [22]. It is good at the simulation of the ducting effect in atmosphere. Wide angle PE [23] and 3D PE [24] are in use but they are not as suitable as the ray tracing method in simulating 3D urban radio propagation.

In the following sections, we will introduce the ray concept, discuss main propagation mechanisms in terms of ray optics, explain basic ray-tracing algorithms and ray-tracing acceleration schemes (software and hardware). Accuracy of the ray tracing is discussed and finally, a perspective for the future of ray tracing is presented.

Some previous review papers related to ray tracing method can be found in [16].

II. THE RAY CONCEPT

The ray concept is very intuitive from our daily experience with the sun light. When the sun light goes through an opening (large compared with wavelengths) on a wall and enters the room, we can see the 'ray' which is propagating along a straight line. More rigorously, the ray concept can be explained using the high frequency approximation of Maxwell's equations, see for example, [25]. The key in this explanation is the assumption that for a propagating wave, the associated electric and magnetic fields can be expressed as:

$$\vec{E}(\vec{r}) = \vec{e}(\vec{r})\, e^{-j\beta_0 S(\vec{r})}$$
$$\vec{H}(\vec{r}) = \vec{h}(\vec{r}) e^{-j\beta_0 S(\vec{r})} \quad (3)$$

where $\vec{e}(\vec{r})$ and $\vec{h}(\vec{r})$ are magnitude vectors and $S(\vec{r})$ is the optical path length or eikonal. Note that they are all functions of $\vec{r}$. Also the time variation in (3) is assumed harmonic and is dropped conventionally.

From Maxwell's equations with $\beta_0 \to \infty$ (high frequency regime) we have Faraday's law, Ampere's law, and Gauss' laws for electric and magnetic fields in free space (without sources):

$$\begin{aligned} \nabla S\times\vec{e}-\mu_r\eta_0\vec{h}&=0\\ \nabla S\times\vec{h}+\varepsilon_r\eta_0\vec{e}&=0\\ \vec{e}\cdot\nabla S&=0\\ \vec{h}\cdot\nabla S&=0 \end{aligned} \tag{4}$$

where, $\eta_0=\sqrt{\frac{\mu_0}{\varepsilon_0}}$ is the impedance of free space.

We can see from the last two equations in (4) that the direction of electric and magnetic field is perpendicular to the normal direction of surfaces formed by $S = const$ (which is the wavefront surface). This normal is also the direction of the propagation direction of energy. Also, from the first equation in (4), we observe that the magnetic field has the direction determined by $\nabla S\times\vec{e}$. Thus, the magnetic field is perpendicular to the electric field as well as the propagation direction. Therefore, the electric field, the magnetic field, and the propagation direction are mutually perpendicular, the same relation as in a plane wave in free space.

Eliminate $\vec{h}$ using the first two equations in (4) and with some vector algebra, we can get the eikonal equation:

$$|\nabla S|^2=n^2 \tag{5}$$

where, $n=\sqrt{\mu_r\varepsilon_r}$ is the index of refraction of the medium.

It can be shown by calculating the time averaged Poynting vector that the power is flowing in the direction perpendicular to the wavefront surface.

To introduce the ray concept, we consider a series of wavefronts. Then we can draw the power flow lines which are perpendicular to these wavefronts. The power lines are the rays and they won't intersect if there is no focus point. Assume ds is a distance element along such a line. Then we can obtain the differential equation describing the power flowing line or the ray trajectory:

$$\frac{d}{ds}\left(n\frac{d\vec{r}}{ds}\right)=\nabla n \tag{6}$$

When the medium is homogeneous, i.e., ε and μ, and n, are constant, we have $\nabla n = 0$ and the ray trajectory equation (7) becomes,

$$\frac{d^2\vec{r}}{ds^2}=0 \tag{7}$$

which has a solution $\vec{r}=\vec{a}s+\vec{b}$ with $\vec{a}$ and $\vec{b}$ being constant vectors. Thus, in homogenous medium, the ray trajectory is a straight line.

It is demonstrated in [25] that Fermat's principle of least time can be proved using the ray concept. From Fermat's principle we can obtain the laws of reflection and refraction, and even the law of diffraction [26].

The ray concept provides an effective means to understand different propagation mechanisms and a visual tool to gain insight of the interaction of EM waves.

For the purpose of radio propagation modeling using ray tracing, we summarize the ray concept as follows:

1) A ray travels in a straight line in homogeneous medium.
2) It obeys the laws of reflection and refraction, as well as the law of diffraction.
3) A ray carries energy. It is more intuitive to treat a ray as a tube (surrounding this central ray) in which the energy is contained and propagated [27].

Fig. 1 shows a ray and the associated ray tubes for a point source. Note that when a ray is traveling, the cross section of the ray tube usually increases such that the total energy or power through the cross section is constant. Equivalently, the energy density on the cross section becomes smaller as the ray travels. This effect 'spreads' the energy out and makes the field smaller when the ray travels further. The so-called *spreading factor* is used to count this effect. The electric field can also be reduced by, e.g., reflection and diffraction.

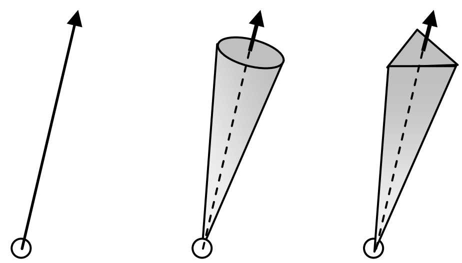

FIGURE 1. A ray (left) and ray tubes with circular (middle) and triangular (right) cross sections for a point source.

The ray concept can also be derived without using the high frequency approximation, see [28], [29].

III. TYPES OF RAYS: PROPAGATION MECHANISMS

When the ray concept is valid, we can describe the EM wave propagation using several mechanisms. For simplicity, we can imagine a point source from which many rays are emanating. Consider one of the rays and based on the behavior of this ray we can classify it as one of the following types of rays.

A. DIRECT RAYS: LINE OF SIGHT PROPAGATION

If the ray goes from the source to the field point directly, it is called a direct ray which is related to line of sight (LoS) propagation mechanism.

B. REFLECTED AND TRANSMITTED RAYS

If a ray is reflected (transmitted) one or more times before reaching the field point, the ray is called a reflected (transmitted) ray. This ray corresponds to the reflection (transmission) of EM waves at interfaces between different mediums. The propagation direction of a reflected (transmitted) ray is determine by the law of reflection (refraction). The magnitude of the reflected (transmitted) field is determined by Fresnel's equations for different polarizations.

C. DIFFRACTED RAYS

Diffracted rays are more complicated compared with the direct, reflected, and transmitted rays. First, one incident ray can spawn many diffracted rays (eg. a continuum cone of rays for diffraction from a wedge). In Fig. 2, the diffracted rays from an edge are shown. For comparison, the reflected ray from an interface of two different mediums is also shown. Second, the calculation of diffraction coefficient is much more complicated than the reflection and transmission coefficients. Third, there are different formulations for the calculation of the diffraction coefficients which may give different field results. These difficulties are the reasons why we may have wide variety of methods for the calculation of diffracted field such as the knife edge method discussed in the previous section.

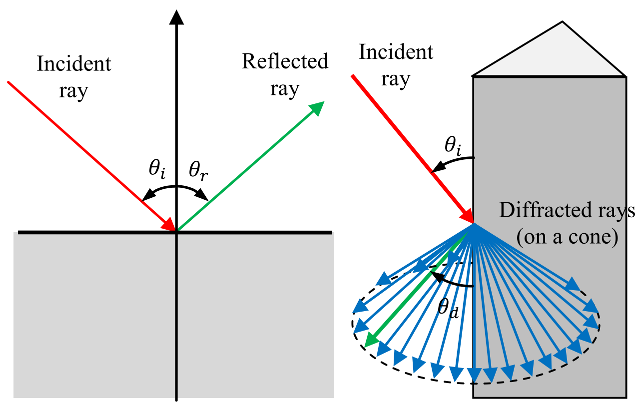

FIGURE 2. **The reflected ray (left) from an planar interface between two different mediums and the diffracted rays (right) from an edge. Note that there is only one single reflected ray but a continuum of diffracted rays (on a cone).**

The development of the geometrical theory of diffraction (GTD) and later the uniform theory of diffraction (UTD) greatly improved the accuracy for diffraction calculation for wedges. The GTD was developed by Keller in 1960's where the Fermat's principle of least time is applied to the determination of the diffracted ray path [26] and the law of diffraction was formulated: the incident angle is equal to the diffraction angle.

A problem with GTD is that its result is not continuous across the shadow boundaries. This problem is solved by the UTD method, pioneered by Kouyoumjian and Pathak [30]. This method has been widely used ever since and computer programs for calculating the diffraction coefficients can be found in textbooks [31]. The original UTD method is valid for perfect electric conductors (PEC). Heuristic methods have been developed to treat lossy wedges [32]–[36]. Other research work has been done for wedges with impedance surfaces [37], [38] and transparent wedges [39]–[41]. The uniform asymptotic theory (UAT) developed in [42] and many related researches [43]–[45] can also provide continuous diffracted field across shadow boundaries, although it is not as widely used as UTD. Comparisons between the two uniform methods can be found in [46] and [47]. Other theories of diffraction exist including the physical optics method [13] and the spectral method [48], [49].

Another difficulty with diffraction field is the determination of the diffraction points when multiple edges are present. Recently, methods for determining the diffracted ray trajectory due to multiple edges in 3D space have been developed [50]–[52]. The method in [52] minimizes the total distance of a diffracted ray path when a sequence of edges is given. The method is especially efficient because the iteration number is usually small.

Calculation of diffraction coefficient for multiple wedges is still a research topic. Analytical solutions for double and triple diffraction coefficients have been developed for arbitrarily oriented 3D wedges [53], [54]. Note that in many practical scenarios, our experience shows that a ray with more than three diffractions is usually not so contributive to the total power received at a field location.

D. SCATTERING

Another propagation mechanism is the *scattering* from rough surfaces such as the ocean surface and building facades. For urban scenarios, the ray concept can still be used by incorporating the effect of scattering or defuse from these objects [55]. The scattering from building facades is divided into specular and nonspecular components [56]. In [57], the importance of incorporating the defuse scattering effect is validated by comparing the ray tracing simulated results with the measurement. The effective roughness concept is proposed in [58] and [59] for the calculation of scattered power form building facades. Recent developments for modeling diffuse scattering of urban environments using ray tracing can be found in [60]. Polarimetric properties of scattered power from building walls are characterized. Polynomial chaos is used in [61] to analyze the scattered field from building facades. Other approaches such as the Green's function method, near and far field method are also used in modeling the scattering from building surfaces [62], [63].

IV. BASIC RAY TRACING ALGORITHMS

A key part of ray tracing methods is to determine the rays from a source location to a field point. In the simplest case, i.e., in free space, the procedure is trivial: there is only one ray present (the direct ray) which is a straight line from the source to the receive point. In an urban environment which is the most common scenario for using ray tracing, there may exist many rays from a source location to a field point; each ray may undergo different number of reflections, diffractions, or their combinations. To determine these rays is not a trivial task but has been a hot research area since the 1990's. It involves two aspects: fast ray-tracing algorithms and accurate field calculations.

In this section we examine the basic ray tracing algorithms which are simple but have the fundamental essence of the ray tracing method.

A. GENERAL THEOREM: FERMAT'S PRINCIPLE OF LEAST TIME

Fermat's principle of least time determines how a ray finds its path traveling from one location to another in a propagation environment. It states that the ray will take a route which consumes the least time possible traveling from one point to another. Based on this principle, the laws of reflection, transmission, and diffraction can be derived. It also leads to the image method which is commonly used to determine the trajectory of reflection rays.

B. IMAGE METHOD

In Fig. 3, when the source (Tx) and the field (Rx) locations are given, the trajectory of a ray reflected from a plane surface (Σ) can be easily determined by the image method. The procedure is as follows. First, locate the image of Rx, Ri, with respect to the planar reflection surface. Second, connect Tx and Ri to obtain a line segment with intersects the plane at a point Q. Then, the reflected ray path is determined by three points (Tx, Q, Rx). Note that we can also take the image of Tx and connect Rx with the image point to obtain the same intersection point Q.

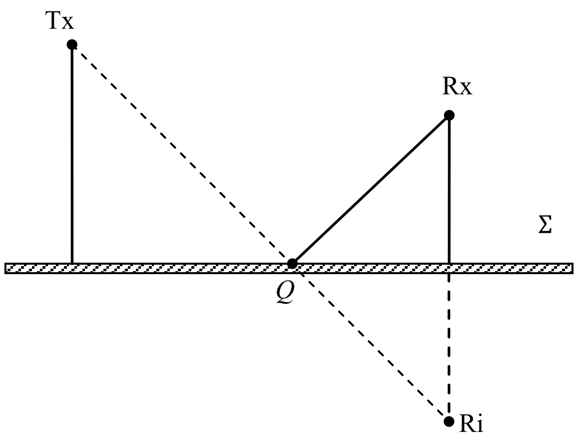

FIGURE 3. **The image method. R_i is the image of R_X with respect to the reflection plane $\sum$.**

The image method can be extended to determine ray path with multiple reflections. The procedure is recursive and can be implemented in a computer program conveniently.

But in a typical urban environment, the pure image method may not be efficient due to the large number of reflection surfaces, leading to slow computation speed. This is one of the reasons that the shooting and bouncing ray method is more widely used in practical propagation modeling.

C. SHOOTING AND BOUNCING RAY (SBR) METHOD

The shooting and bouncing ray method was first introduced in [64] for the calculation of radar cross section of cavities. It has been used in radio propagation modeling ever since.

The basic idea of SBR is to trace every ray launched from a source location to determine if they arrive at a field point. It has three steps: ray launching, ray tracing, and ray reception.

For ray launching, it is usually required that all the rays emanating from the source point to be as uniformly distributed as possible so that each ray carries similar power for an isotropic source. This involves the uniform division of a spherical surface. It is well known that the finest uniform division is the regular icosahedron with 20 identical equilateral triangular faces and 12 vertices. Finer division of the sphere will lead to non-uniform cross-sections of the ray tubes. In practice, this issue does not cause significant accuracy problems, and ray tracing methods can provide satisfactory path loss results (compared with measured path loss results).

When a ray is traced from the source location, it can go to the field point directly, or it can be reflected and diffracted several times before reaching the field point. In a typical urban environment, this procedure involves an important step: determining if the ray intersects any object in the scene. If the ray hits an object, a reflected or diffracted ray will be spawned. This ray-object intersection tests usually consumes more than 90% of computational time in a non-sophisticated implementation of the ray tracing algorithms [65]. Significant research work has been done in accelerating the ray tracing algorithms which will be discussed in Section V.

The third step is the reception test for a ray. A ray is associated with a ray tube with an increasing cross-section area as the ray travels. When the ray tube illuminates the receiving point, the ray is received and the respective field can be calculated. Thus, the reception of a ray is the test that determines whether the field point is inside the ray tube. There are two types of ray tubes. One has a circular cross section while the other is polygonal. The circular cross-section ray tube is easy to implement but may cause ray double counting [66]. For polygonal (usually triangular) cross-section ray tubes, ray double counting is not an issue, but three or more rays have to be traced simultaneously in order to trace the tube, which may adversely affect the computational speed and programming complexity.

D. HYBRID METHOD

Although the SBR method is simple to implement, the ray trajectory may be not as exact as determined by the image method. In [67], a hybrid method is proposed which takes the advantages of SBR (faster computation speed) and the image methods (accurate ray path). This method first uses the SBR method to determine a valid ray (received by the Rx). Then the image method is employed to adjust the ray trajectory. Since we know all the reflecting surfaces associated with this ray, the image method only needs to determine the images of Tx or Rx with respect to these reflecting surfaces in a known sequence. Therefore, the image method can be very fast in this procedure and due to the fact that the number of received rays is usually much smaller than that of launched rays, the overhead of using image method for improving the accuracy of ray paths is negligible.

V. ACCELERATION METHODS

The implementation of the SBR algorithm has been an important research area. Many strategies have been studied to achieve better computational efficiency. We will discuss three main schemes in this section to illustrate how significant acceleration can be realized.

A. SPACE DIVISIONS

This method is a preprocess procedure which divides the entire propagation environment into small cells. These cells have explicit or implicit information of their neighbors. When a ray traversing the environment is currently residing in a cell, the next cell the ray enters can be determined by looking up the neighboring information. This scheme reduces the number of candidate objects for the ray-object intersection tests and accelerates the computational speed.

There are several approaches using the space division methods.

1) UNIFORM DIVISION

The entire space of interest is divided into a uniform grid with identical cells. The cell size is constant, e.g., $dx \times dy \times dz$ for a rectangular division in three dimensional scenarios. In the preprocess, the objects in the scene will have the cells to which they belong determined and for each cell, the objects contained in the cell are calculated.

When a ray is traversing the scene, it traverses the uniform gird. In computer graphics, this traversing is well studied and fast algorithms exist. An example can be found in [68] and an application in radio propagation modeling in [69].

The key step in this algorithm is to identify the next cell the ray enters. For simplicity, we take a two-dimensional example. Assume the cell size is $\Delta_x \times \Delta_y$ and a cell is labeled by $C(i, j)$ as shown in Fig. 4. The grid lines are located at $x = i \times \Delta_x$ for vertical lines and at $y = j \times \Delta_y$ for horizontal lines.

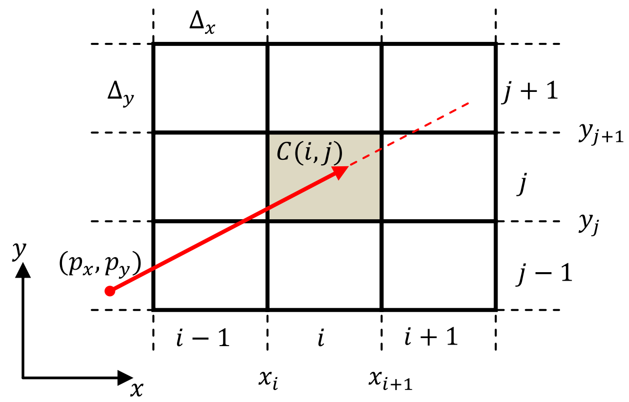

FIGURE 4. A rectangular grid. Each cell is a rectangle. A ray is currently residing in the cell $C(i, j)$.

For a given ray, the ray direction can be defined by a unit vector (a_x, a_y). Then we can define two lengths:

$$D_x = \frac{\Delta_x}{a_x}, \quad D_y = \frac{\Delta_y}{a_y} \tag{8}$$

for $a_x \neq 0$, $a_y \neq 0$. Note that D_x is the length of the ray trajectory cut by two vertical adjacent grid lines $x = x_i$ and $x = x_{i+1}$ and D_y is the length of the ray trajectory cut by two horizontal adjacent grid lines $y = y_j$ and $y = y_{j+1}$.

Then we keep two distances dx and dy which will be updated and compared to determine which cell the ray enters next from the current cell the ray is residing. Assume the source point is located at (p_x, p_y). Then the initial value of $dx = dx_0$ is the ray length cut by two lines $x = p_x$ and $x = x_m$ (the first vertical grid line that the ray hits); the initial value of $dy = dy_0$ is the ray length cut by two lines $y = p_y$ and $y = y_n$ (the first horizontal grid line the ray hits).

The algorithm for the ray traversing can now be expressed in terms of a comparison between dx and dy:

If $dx > dy$, a horizontal grid line is traversed. The ray will go to the cell upward (or downward depending on the ray direction); update dy with $dy + D_y$;

Else if $dy > dx$, a vertical grid line is traversed. The ray will go to the cell left (or right depending on the ray direction); update dx with $dx + D_x$.

The procedure repeats for the updated dx and dy values until some stop criterion is met.

The traversing algorithm is very fast because it only involves one addition and one comparison at each step. For each cell, the ray will be tested for intersection with any of the objects in the cell.

The rectangular grid method is extremely efficient if all the objects are aligned with the grid lines as discussed in [69].

2) BOUNDING VOLUME HIERARCHY (BVH)

The efficiency of uniform division may degrade when the objects are distributed non-uniformly. The BVH method is trying to divide the scene into bounding volumes which are structured with different sizes and topological relations. Thus, the bounding volumes may be large if few objects exist in that region. On the other hand, if there are many objects in a region, more bounding boxes with smaller sizes may be added. A widely used such method is the k-d (k-dimensional) tree algorithm. This is also a well studied topic in computer graphics for ray tracing [70], [71].

To create the k-d tree, we can take a 2D example ($k = 2$). The root of the tree is the entire scene. Then a vertical line ($x = x_1$) is drawn which divides the scene into two parts (left and right). We then draw a horizontal line $y = y_1^L$ for the left part and a line $y = y_1^R$ for the right part to divide each of these two parts into two smaller cells. Then for each of these four cells, repeat the process until the stop condition is met. A k-d tree is a binary tree which means that for each node there we can have a left and a right sub-node.

A good k-d tree is depending on how to determine the location of partitioning lines (or hyper planes in general cases). In general, the partition line is not the one that equally divides the region. The surface area heuristic (SAH) is a valuable method for this choosing the partition lines [69] where the k-d tree with SAH is used for radio propagation modeling for an indoor environment.

Similar to k-d tree, the binary partition, the quadtree, and octree are also used in dividing the propagation scenes. They are less sophisticated but simpler to implement.

3) OTHER SPACE DIVISION METHODS

There are many other space division methods for radio propagation modeling. The triangular grid method divides the 2D ground projection of buildings into a mesh of triangles. The projected buildings form a planar straight line graph (PSLG) [72] which requires the triangulation to keep all the segments (projected walls) intact. A constrained Delaunay triangulation is then performed and no existing segments (walls) are divided into sub-segments. Thus, all the added edges for the triangulation are not real walls.

In this triangular mesh, each triangle has the information about its three neighbors with respect to its three edges and each vertex has a list of triangles which fan about this vertex. When a ray is traversing the mesh, it is easy to identify the next triangle the ray will enter with such information. This is because there are only two possible choices for a ray in the current triangle to enter the next triangle: the two edges the ray is going to cross (assuming the ray enters the current triangle by crossing the third edge). More details can be found in [16], [73]–[75]. In [72], a very fast and excellent quality program for building the triangular mesh can be downloaded free. Other space division methods such as the angular Z-Buffer (AZB) method can be found in [16], [65], and [76]. In [77], in order to speed up the ray tracing simulation, an 'active part' of the propagation environment is identified and used as the input environmental model. This can significantly reduce the size of the simulation problem without loss of accuracy of simulation results.

B. TWO-DIMENSIONAL SIMPLIFICATION

In many cases the 3D propagation scene can be simplified to a 2D environment with some special treatment. The reduction from 3D to 2D usually guarantees significant speedups in computation. The triangular grid method mentioned in the previous sub-section is such an example. When the trajectory of a ray is found in the 2D triangular mesh, the corresponding 3D ray path can be determined since the heights of the transmitter and receiver are known. Also the roof top diffracted rays can be calculated approximately using the triangular grid and the building height information [73].

In [78], a 2D/2.5D method is proposed and the simulated results compare very well with the measured results. Another 2D method, the vertical plane launch (VPL) method, is quite different from the ground-projected 2D methods [79]. In VPL method, vertical half-planes are used to determine the reflection and diffraction points. A vertical plane will intersect building walls and rooftops. Then all the rays contained in this plane can be tested to determine if any reflection or diffraction happens. When reflection occurs, for example, a new vertical half-plane which contains the reflected ray will be used to find the intersected buildings of the reflected ray. This procedure repeats until some stop criterion is met. It is shown in [80] that the VPL method has very good accuracy when the mean height of building is about the height of the transmitter.

Other acceleration methods not belonging to space division and 2D simplification exist such as the ray-path search algorithm [81], [82]. This method exploits the visibility of building surfaces to avoid unnecessary ray-object intersection tests. Another method uses the concept of illumination zone to limit the ray-object tests [83], [84] and accelerates the ray tracing procedure. One disadvantage of these methods is that it is Tx location dependent.

C. GPU ACCELERATION

In the past decade, graphics processing units (GPU) have been a hot research topic in accelerating the computational speed for many applications. GPU's are massively multithreaded many-core chips and appear in computer video cards and embedded systems. They are created mainly for graphics computations such as polygon rendering, coordinate transformations for vertices of geometrical objects, and texture mapping. As GPU's become more powerful and sophisticated, they have been found in applications not related to computer graphics. They can speed up some numerical methods such as the finite-difference time-domain method by tens or hundreds of times.

For ray tracing, the early uses of GPU for acceleration also starts in computer graphics.

Recently, GPU's have been introduced to the ray tracing method for radio propagation modeling. In [85] and [86], a beam tracing method is developed using GPU acceleration for 2D propagation modeling. Significant speedups are achieved (computational time reduced from minutes to seconds). Although beam tracing contributed to part of the speedups, the GPU's are the main benefactor. A 3D beam tracing method using GPU acceleration is discussed in [87] for an indoor propagation environment. In [88], the GPU acceleration technique is used for a 3D ray tracer for urban environments. In [89], a general purpose ray tracing engine, OptiX, is developed by NVIDIA. OptiX is a programmable system specifically designed for NVIDIA's GPU. It is free and can be tunable for different uses. Although most applications of OptiX are in computer graphics, recently, it has been used to accelerate ray tracing for radio propagation modeling [89]. The authors of [90] have shown that OptiX helps find more valid rays than their in-house ray tracing software for the same depth of reflections and with reduced simulation time.

VI. ACCURACY AND OTHER DEVELOPMENT OF RAY TRACING AND PROPAGATION MODELING

The ray tracing method has been widely used in radio propagation modeling and simulation. In this section we discuss the accuracy and recent development of propagation modeling related to ray tracing methods.

Compared with measured results, ray tracing methods can provide satisfactory accuracy for path loss predictions [91], [92]. The ray tracing results are especially accurate when comparing the general tendency of simulated path loss (or the signal levels) with the measured results [78].

Thus, an average process is usually used to filter out the sensitive local variations of the predicted results when the ray fields are added coherently. This is similar to the measurement process where mean received power is obtained by averaging the received signal along a line (straight or circular) or over an area to filter out the small scale fading [93], [94]. Ray tracing can also provide angle of arrival/departure, delay profile, and wideband results with good accuracy [57].

There are many path loss measurement campaigns. One widely cited measured result is introduced in the European COST 231 project [15]. The measurements were made by the German GSM network operator Mannesmann Mobilfunk GmbH in downtown Munich, Germany. The measurement involved an area of $2.4 \times 3.4\ \mathrm{km}^2$. The path loss values along three different routes are reported. Many ray tracing publications compare their simulated results with these measured results to validate their accuracy. Another example of well known measurement results can be found in [79].

The accurate modeling of the propagation environments plays an important role in the accuracy of the propagation modeling using ray tracing methods. For the urban scenarios, the building footprints and heights are usually known within limited accuracy. In [95], the effect of different building databases on ray tracing results is examined. In [96], it is reported that the building footprints can have one meter error without affecting the predicted path loss values. The effect of building footprints and heights on the ray tracing results are also reported in [97] and [98].

Recently, as the geospatial data are getting popular in applications such as in Google Earth and Google Maps, it is common to use web services to view 3D building structures online for many cities. It is then interesting if these 3D buildings can be extracted for propagation modeling. In [97] and [99], using 2D images of the 3D buildings from Google Earth it is shown that the 3D buildings can be reconstructed with good accuracy. In [100], machine learning is used to rebuild 3D urban scenarios. With appropriate training, the machine learning algorithm can reconstruct large scales of buildings with satisfactory accuracy.

Digital elevation databases are also used to represent the terrain involved in propagation modeling. NASA's SRTM (Shuttle Radar Topography Mission) [101] database is one of the publically available resources. It has digital elevation data covering about 80 % of the earth's landmass. The database is composed of about 14,000 files each covers a 1×1 degree area. Typical resolution is 3 arc second (around 90 - 100 meters). SRTM data can also be obtained from USGS (U. S. Geological Survey) which distributes both "unfinished" and "finished" grade versions of the elevation data [102]. Another free elevation database is the National Elevation Dataset (NED) available from USGS [103]. It has many levels of resolution (from around 60 meters to 1 meter) covering different regions. It is also possible to extract terrain elevation data from free software such as the Google Earth using their built-in functions or API's (Application Programming Interface). In [104], using Google Earth's API which returns elevation data and latitude/longitude values for each pixel in the scenes, terrain elevation data are extracted on a grid and used in the propagation simulation.

As more and more digital elevation data are available with better resolutions, it is getting more convenient to extract terrain features important for radio propagation modeling such as the mountain peaks and ridges. In [105], a simple method is used to extract 3D ridges from digital elevation data. The extracted ridges then serve as diffraction wedges in simulating the radio wave propagation. It is shown that 3D features of ridges, e.g., the orientation and elevation parameters, are necessary for accurate calculation of diffracted field. These 3D features are commonly ignored in widely used propagation modeling methods such as the knife edge diffraction. For multiple diffractions, the 3D features of ridges and their effect on the diffraction are investigated in [106].

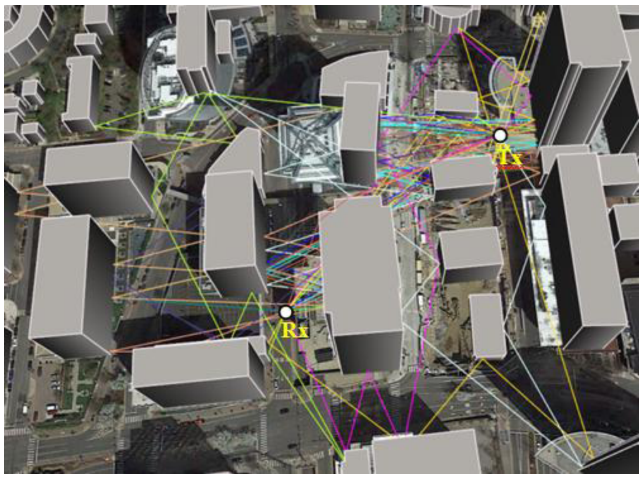

FIGURE 5. Three-dimensional buildings and rays from T_X to R_X are rendered in Google Earth. The photo-realistic background provided by Google Earth enhances the visual feel. A user can rotate the scene and zoom in/out to examine the 3D ray structures.

With LIDAR (Light Detection and Ranging), much finer resolution can be obtained. LIDAR has been used for reconstruction of 3D buildings in urban areas, see examples at the USGS website [107]. With these finer environmental modeling tools and means available, it is expected more complex propagation environment can be modeled more realistically and more accurate radio propagation predictions can be achieved. It is also useful to render the propagation results in some map software such as Google Earth. In Fig. 5, the 3D buildings and rays from the transmitter Tx to the receiver Rx are displayed in Google Earth which provides a photo-realistic environment. Using Google Earth's functions, one can rotate the scene and zoom in/out for careful examination of the ray trajectories.

VII. CONCLUSION AND A FUTURE PERSPECTIVE

Radio propagation modeling is a key part in the design of wireless communication systems. In the past several decades, great research and application work have been done and many useful models and techniques have been developed.

In the near future, the radio propagation modeling will be further developed to achieve intelligent, accurate, and real time application goals.

First, as an integral part of the simulation system, the geospatial databases will have higher resolution and different levels of detail of the propagation environment will be available or can be derived on fly in the simulation process. Second, the simulation will be intelligent in determining which level-of-detail environment is to be used based on parameters such as the propagation range, frequency, and antenna types. Third, different modeling algorithms will be integrated and the most suitable model will be employed to simulate the radio wave propagation to accommodate the requirement of communication system under consideration. Fourth, faster computation speed will be achieved by using hardware acceleration and new algorithms. Together, these features will lead to real-time simulation speed with capability of simulating a large variety of propagation scenarios. Also, the simulation system will be easy to use and will cost less.

Technologies such as machine learning and big data inference will help build such a system which is ‘wise’ enough to make simulation fast and accurate. Using machine learning, for example, the system will be able to identify features of propagation environment such as cities, rural areas, mountain ridges, etc., and determine suitable levels of detail of the environmental model.

With real-time capability and geospatial awareness, the propagation prediction can be used in many wireless communication systems to enhance their performance. For example, in cognitive radio, real time radio map is needed to determine the spectrum availability [108]. This can be achieved with the future propagation modeling tool when the mobile unit is equipped with GPS.

Ray tracing, as a more recent method for propagation modeling, has undergone tremendous progress and has been proved useful. Ray tracing is a more general method than other methods such as the empirical models. It has a sound physical basis (high frequency solution of Maxwell’s equation) and can be applied to many of the propagation scenarios in wireless communications.

Ray tracing will play an important role in the future propagation modeling tools. In our opinion, the ray tracing method, integrated with empirical and other numerical methods (e.g., parabolic equation method), can serve as the backbone of the intelligent modeling system. It will be most useful for tackling complicated propagation environments in high frequency regimes. As pointed out in [109], ray tracing method will be embedded in wireless communication systems to provide real-time channel estimation.

REFERENCES

[1] W. Gordon, “A hundred years of radio propagation,” *IEEE Trans. Antennas Propag.*, vol. 33, no. 2, pp. 126–130, Feb. 1985.

[2] Ericsson. Stockholm, Sweden. (Nov. 2014). *Ericsson Mobility Report*. [Online]. Available: http://www.ericsson.com/res/docs/2014/ericsson-mobility-report-november-2014.pdf

[3] H. T. Friis, “A note on a simple transmission formula,” *Proc. IRE*, vol. 34, no. 5, pp. 254–256, May 1946.

[4] J. Keller, “One hundred years of diffraction theory,” *IEEE Trans. Antennas Propag.*, vol. 33, no. 2, pp. 123–126, Feb. 1985.

[5] K. Bullington, “Radio propagation at frequencies above 30 megacycles,” *Proc. IRE*, vol. 35, no. 10, pp. 1122–1136, Oct. 1947.

[6] *Propagation by Diffraction*, document Rec. ITU-R P.526-12, 2012. [Online]. Available: http://www.itu.int

[7] J. Epstein and D. W. Peterson, “An experimental study of wave propagation at 850 Mc,” *Proc. IRE*, vol. 41, no. 5, pp. 595–611, May 1953.

[8] J. Deygout, “Multiple knife-edge diffraction of microwaves,” *IEEE Trans. Antennas Propag.*, vol. 14, no. 4, pp. 480–489, Jul. 1966.

[9] C. L. Giovaneli, “An analysis of simplified solutions for multiple knife-edge diffraction,” *IEEE Trans. Antennas Propag.*, vol. 32, no. 3, pp. 297–310, Mar. 1984.

[10] G. A. Hufford, A. G. Longley, and W. A. Kissick. (Apr. 1982). A guide to the use of the ITS irregular terrain model in the area prediction mode. U.S. Department of Commerce, Washington, DC, USA. [Online]. Available: http://www.ntia.doc.gov/files/ntia/publications/ntia_82-100_20121129145031_555510.pdf

[11] M. Hatay, “Empirical formula for propagation loss in land mobile radio services,” *IEEE Trans. Veh. Technol.*, vol. 29, no. 3, pp. 317–325, Aug. 1980.

[12] Y. Okumura, E. Ohmori, T. Kawano, and K. Fukuda, “Field strength and its variability in VHF and UHF land-mobile service,” *Rev. Elect. Commun. Lab.*, vol. 16, nos. 9–10, pp. 825–873, 1968.

[13] H. L. Bertoni, *Radio Propagation for Modern Wireless Systems*. Upper Saddle River, NJ, USA: Prentice-Hall, 2000.

[14] T. S. Rappaport, *Wireless Communications: Principles and Practice*, 2nd ed. Upper Saddle River, NJ, USA: Prentice-Hall, 2002.

[15] E. Damosso and L. M. Coreia, *COST Action 231: Digital Mobile Radio Towards Future Generation Systems: Final Report*, European Commission, 1999.

[16] M. F. Iskander and Z. Yun, “Propagation prediction models for wireless communication systems,” *IEEE Trans. Microw. Theory Techn.*, vol. 50, no. 3, pp. 662–673, Mar. 2002.

[17] A. Taflove and S. C. Hagness, *Computational Electrodynamics: The Finite-Difference Time-Domain Method*, 3rd ed. Norwood, MA, USA: Artech House, 2005.

[18] J.-M. Jin, *The Finite Element Method in Electromagnetics*, 2nd ed. New York, NY, USA: Wiley, 2002.

[19] R. F. Harrington, *Field Computation by Moment Methods*. New York, NY, USA: Wiley, 1993.

[20] G. D. Dockery, “Modeling electromagnetic wave propagation in the troposphere using the parabolic equation,” *IEEE Trans. Antennas Propag.*, vol. 36, no. 10, pp. 1464–1470, Oct. 1988.

[21] A. E. Barrios, “Parabolic equation modeling in horizontally inhomogeneous environments,” *IEEE Trans. Antennas Propag.*, vol. 40, no. 7, pp. 791–797, Jul. 1992.

[22] A. E. Barrios, “A terrain parabolic equation model for propagation in the troposphere,” *IEEE Trans. Antennas Propag.*, vol. 42, no. 1, pp. 90–98, Jan. 1994.

[23] R. J. Kuttler, “Differences between the narrow-angle and wide-angle propagators in the split-step Fourier solution of the parabolic wave equation,” *IEEE Trans. Antennas Propag.*, vol. 47, no. 7, pp. 1131–1140, Jul. 1999.

[24] K. B. Thiem, “A 3D parabolic equation based technique for predicting propagation path loss in an urban area,” M.S. thesis, Naval Postgraduate School, Monterey, CA, USA, Sep. 2001.

[25] M. Born and E. Wolf, *Principles of Optics: Electromagnetic Theory of Propagation, Interference and Diffraction of Light*, 7th ed. Cambridge, U.K.: Cambridge Univ. Press, 1999.

[26] J. B. Keller, “Geometrical theory of diffraction,” *J. Opt. Soc. Amer.*, vol. 32, no. 2, pp. 116–130, Feb. 1962.

[27] L. B. Felsen and N. Marcuvitz, *Radiation and Scattering of Waves*. Hoboken, NJ, USA: Wiley, 2003.

[28] R. K. Luneburg, *Mathematical Theory of Optics*. Berkeley, CA, USA: Univ. California Press, 1966.

[29] M. Kline and I. W. Kay, *Electromagnetic Theory and Geometrical Optics*. New York, NY, USA: Interscience, 1965.

[30] R. G. Kouyoumjian and P. H. Pathak, “A uniform geometrical theory of diffraction for an edge in a perfectly conducting surface,” *Proc. IEEE*, vol. 62, no. 11, pp. 1448–1461, Nov. 1974.

[31] C. A. Balanis, *Advanced Engineering Electromagnetics*. New York, NY, USA: Wiley, 1989.
[32] R. J. Luebbers, "Finite conductivity uniform GTD versus knife edge diffraction in prediction of propagation path loss," *IEEE Trans. Antennas Propag.*, vol. 32, no. 1, pp. 70–76, Jan. 1984.
[33] R. J. Luebbers, "Comparison of lossy wedge diffraction coefficients with application to mixed path propagation loss prediction," *IEEE Trans. Antennas Propag.*, vol. 36, no. 7, pp. 1031–1034, Jul. 1988.
[34] P. D. Holm, "A new heuristic UTD diffraction coefficient for nonperfectly conducting wedges," *IEEE Trans. Antennas Propag.*, vol. 48, no. 8, pp. 1211–1219, Aug. 2000.
[35] C. Tzaras and S. R. Saunders, "An improved heuristic UTD solution for multiple-edge transition zone diffraction," *IEEE Trans. Antennas Propag.*, vol. 49, no. 12, pp. 1678–1682, Dec. 2001.
[36] P. Bernardi, R. Cicchetti, and O. Testa, "A three-dimensional UTD heuristic diffraction coefficient for complex penetrable wedges," *IEEE Trans. Antennas Propag.*, vol. 50, no. 2, pp. 217–224, Feb. 2002.
[37] R. Tiberio, G. Pelosi, and G. Manara, "A uniform GTD formulation for the diffraction by a wedge with impedance faces," *IEEE Trans. Antennas Propag.*, vol. 33, no. 8, pp. 867–873, Aug. 1985.
[38] R. G. Rojas, "Electromagnetic diffraction of an obliquely incident plane wave field by a wedge with impedance faces," *IEEE Trans. Antennas Propag.*, vol. 36, no. 7, pp. 956–970, Jul. 1988.
[39] C. Demetrescu, C. C. Constantinou, and M. J. Mehler, "Scattering by a right-angled lossy dielectric wedge," *IEE Proc.-Mricow., Antennas Propag.*, vol. 144, no. 5, pp. 392–396, Oct. 1997.
[40] K. A. Remley, A. Weisshaar, and H. R. Anderson, "Improved diffraction coefficients for lossy dielectric wedges," *Electron. Lett.*, vol. 35, no. 21, pp. 1826–1827, Oct. 1999.
[41] C. Demeterscu, B. V. Budaev, C. C. Constantinou, and M. J. Mehler, "TM electromagnetic scattering by a transparent wedge with resistive faces," *IEEE Trans. Antennas Propag.*, vol. 47, no. 1, pp. 47–54, Jan. 1999.
[42] D. S. Ahluwalia, R. M. Lewis, and J. Boersma, "Uniform asymptotic theory of diffraction by a plane screen," *SIAM J. Appl. Math.*, vol. 16, no. 4, pp. 783–807, 1968.
[43] S.-W. Lee and G. A. Deschamps, "A uniform asymptotic theory of electromagnetic diffraction by a curved wedge," *IEEE Trans. Antennas Propag.*, vol. 24, no. 1, pp. 25–34, Jan. 1976.
[44] S. W. Lee, "Uniform asymptotic theory of electromagnetic edge diffraction: A review," in *Electromagnetic Scattering*, P. L. E. Uslenghi, Ed. New York, NY, USA: Academic, 1978, pp. 67–119.
[45] T. B. A. Senior and J. L. Volakis, "Scattering by an imperfect right-angled wedge," *IEEE Trans. Antennas Propag.*, vol. 34, no. 5, pp. 681–688, May 1986.
[46] J. Boersma and Y. Rahmat-Samii, "Comparison of two leading uniform theories of edge diffraction with the exact uniform asymptotic solution," *Radio Sci.*, vol. 15, no. 6, pp. 1179–1194, 1980.
[47] G. A. Deschamps, J. Boersma, and S.-W. Lee, "Three-dimensional half-plane diffraction: Exact solution and testing of uniform theories," *IEEE Trans. Antennas Propag.*, vol. 32, no. 3, pp. 264–271, Mar. 1984.
[48] Y. Rahmat-Samii and R. Mittra, "A spectral domain interpretation of high frequency diffraction phenomena," *IEEE Trans. Antennas Propag.*, vol. 25, no. 5, pp. 676–687, Sep. 1977.
[49] A. Ciarkowski, J. Boersma, and R. Mittra, "Plane-wave diffraction by a wedge—A spectral domain approach," *IEEE Trans. Antennas Propag.*, vol. 32, no. 1, pp. 20–29, Jan. 1984.
[50] E. Di Giampaolo and F. Bardati, "Analytical model of multiple wedge-diffracted ray congruence," *Electromagnetics*, vol. 23, no. 6, pp. 509–523, 2003.
[51] P. Bagnerini, A. Buffa, and A. Cangiani, "A fast algorithm for determining the propagation path of multiple diffracted rays," *IEEE Trans. Antennas Propag.*, vol. 55, no. 5, pp. 1416–1422, May 2007.
[52] G. Carluccio and M. Albani, "An efficient ray tracing algorithm for multiple straight wedge diffraction," *IEEE Trans. Antennas Propag.*, vol. 56, no. 11, pp. 3534–3542, Nov. 2008.
[53] M. Albani, "A uniform double diffraction coefficient for a pair of wedges in arbitrary configuration," *IEEE Trans. Antennas Propag.*, vol. 53, no. 2, pp. 702–710, Feb. 2005.
[54] G. Carluccio, F. Puggelli, and M. Albani, "A UTD triple diffraction coefficient for straight wedges in arbitrary configuration," *IEEE Trans. Antennas Propag.*, vol. 60, no. 12, pp. 5809–5817, Dec. 2012.
[55] V. Degli-Esposti, "A diffuse scattering model for urban propagation prediction," *IEEE Trans. Antennas Propag.*, vol. 49, no. 7, pp. 1111–1113, Jul. 2001.
[56] P. Pongsilamanee and H. L. Bertoni, "Specular and nonspecular scattering from building facades," *IEEE Trans. Antennas Propag.*, vol. 52, no. 7, pp. 1879–1889, Jul. 2004.
[57] F. Fuschini, H. El-Sallabi, V. Degli-Esposti, L. Vuokko, D. Guiducci, and P. Vainikainen, "Analysis of multipath propagation in urban environment through multidimensional measurements and advanced ray tracing simulation," *IEEE Trans. Antennas Propag.*, vol. 56, no. 3, pp. 848–857, Mar. 2008.
[58] V. Degli-Esposti, F. Fuschini, E. M. Vitucci, and G. Falciasecca, "Measurement and modelling of scattering from buildings," *IEEE Trans. Antennas Propag.*, vol. 55, no. 1, pp. 143–153, Jan. 2007.
[59] J. S. Lu, H. L. Bertoni, and V. Degli-Esposti, "Scale model investigation of mechanisms for scattering from office buildings at 2 GHz," *IEEE Trans. Antennas Propag.*, vol. 62, no. 12, pp. 6435–6442, Dec. 2014.
[60] E. M. Vitucci, F. Mani, V. Degli-Esposti, and C. Oestges, "Polarimetric properties of diffuse scattering from building walls: Experimental parameterization of a ray-tracing model," *IEEE Trans. Antennas Propag.*, vol. 60, no. 6, pp. 2961–2969, Jun. 2012.
[61] P. Kersaudy, S. Mostarshedi, B. Sudret, O. Picon, and J. Wiart, "Stochastic analysis of scattered field by building facades using polynomial chaos," *IEEE Trans. Antennas Propag.*, vol. 62, no. 12, pp. 6382–6393, Dec. 2014.
[62] S. Mostarshedi, E. Richalot, J.-M. Laheurte, M.-F. Wong, J. Wiart, and O. Picon, "Fast and accurate calculation of scattered electromagnetic fields from building faces using Green's functions of semi-infinite medium," *IET Microw., Antennas Propag.*, vol. 4, no. 1, pp. 72–82, Jan. 2010.
[63] Y. B. Ouattara, S. Mostarshedi, E. Richalot, J. Wiart, and O. Picon, "Near- and far-field models for scattering analysis of buildings in wireless communications," *IEEE Trans. Antennas Propag.*, vol. 59, no. 11, pp. 4229–4238, Nov. 2011.
[64] H. Ling, R.-C. Chou, and S.-W. Lee, "Shooting and bouncing rays: Calculating the RCS of an arbitrarily shaped cavity," *IEEE Trans. Antennas Propag.*, vol. 37, no. 2, pp. 194–205, Feb. 1989.
[65] M. F. Catedra, J. Perez, F. S. de Adana, and O. Gutierrez, "Efficient ray-tracing techniques for three-dimensional analyses of propagation in mobile communications: Application to picocell and microcell scenarios," *IEEE Antennas Propag. Mag.*, vol. 40, no. 2, pp. 15–28, Apr. 1998.
[66] G. Durgin, N. Patwari, and T. S. Rappaport, "Improved 3D ray launching method for wireless propagation prediction," *Electron. Lett.*, vol. 33, no. 16, pp. 1412–1413, 1997.
[67] S. Y. Tan and H. S. Tan, "A microcellular communications propagation model based on the uniform theory of diffraction and multiple image theory," *IEEE Trans. Antennas Propag.*, vol. 44, no. 10, pp. 1317–1326, Oct. 1996.
[68] J. G. Cleary and G. Wyvill, "Analysis of an algorithm for fast ray tracing using uniform space subdivision," *Vis. Comput.*, vol. 4, no. 2, pp. 65–83, 1988.
[69] Z. Yun, M. F. Iskander, and Z. Zhang, "Fast ray tracing procedure using space division with uniform rectangular grid," *Electron. Lett.*, vol. 36, no. 10, pp. 895–897, May 2000.
[70] I. Wald, "Realtime ray tracing and interactive global illumination," Ph.D. dissertation, Comput. Graph. Group, Saarland Univ., Saarbrücken, Germany, 2004.
[71] I. Wald and W. Havran, "On building fast kd-trees for ray tracing, and on doing that in O(N log N)," in *Proc. IEEE Symp. Interact. Ray Tracing*, Sep. 2006, pp. 61–69.
[72] J. R. Shewchuk. *Triangle: A Two-Dimensional Quality Mesh Generator and Delaunay Triangulator*. [Online]. Available: https://www.cs.cmu.edu/~quake/triangle.html, accessed Jul. 15, 2015.
[73] Z. Yun, Z. Zhang, and M. F. Iskander, "A ray-tracing method based on the triangular grid approach and application to propagation prediction in urban environments," *IEEE Trans. Antennas Propag.*, vol. 50, no. 5, pp. 750–758, May 2002.
[74] Z. Zhang, Z. Yun, and M. F. Iskander, "Ray tracing method for propagation models in wireless communication systems," *Electron. Lett.*, vol. 36, no. 5, pp. 464–465, Mar. 2000.
[75] S. F. Fortune, D. M. Gay, B. W. Kernighan, O. Landron, R. A. Valenzuela, and M. H. Wright, "WISE design of indoor wireless systems: Practical computation and optimization," *IEEE Comput. Sci. Eng.*, vol. 2, no. 1, pp. 58–68, Spring 1995.

[76] F. S. de Adana, O. G. Blanco, I. G. Diego, J. P. Arriaga, and M. F. Catedra, "Propagation model based on ray tracing for the design of personal communication systems in indoor environments," *IEEE Trans. Veh. Technol.*, vol. 49, no. 6, pp. 2105–2112, Nov. 2000.

[77] V. Degli-Esposti, F. Fuschini, E. M. Vitucci, and G. Falciasecca, "Speed-up techniques for ray tracing field prediction models," *IEEE Trans. Antennas Propag.*, vol. 57, no. 5, pp. 1469–1480, May 2009.

[78] K. Rizk, J. Wagen, and F. Gardiol, "Two-dimensional ray-tracing modeling for propagation prediction in microcellular environments," *IEEE Trans. Veh. Technol.*, vol. 46, no. 2, pp. 508–518, May 1997.

[79] G. Liang and H. L. Bertoni, "A new approach to 3-D ray tracing for propagation prediction in cities," *IEEE Trans. Antennas Propag.*, vol. 46, no. 6, pp. 853–863, Jun. 1998.

[80] K. Rizk, R. Valenzuela, S. Fortune, D. Chizhik, and F. Gardiol, "Lateral, full-3D and vertical plane propagation in microcells and small cells," in *Proc. 48th IEEE Veh. Technol. Conf.*, vol. 2. May 1998, pp. 998–1003.

[81] F. A. Agelet, F. P. Fontan, and A. Formella, "Fast ray tracing for microcellular and indoor environments," *IEEE Trans. Magn.*, vol. 33, no. 2, pp. 1484–1487, Mar. 1997.

[82] F. A. Agelet, A. Formella, J. M. H. Rabanos, F. I. de Vicente, and F. P. Fontan, "Efficient ray-tracing acceleration techniques for radio propagation modeling," *IEEE Trans. Veh. Technol.*, vol. 49, no. 6, pp. 2089–2104, Nov. 2000.

[83] M. C. Lawton and J. P. McGeehan, "The application of a deterministic ray launching algorithm for the prediction of radio channel characteristics in small-cell environments," *IEEE Trans. Veh. Technol.*, vol. 43, no. 4, pp. 955–969, Nov. 1994.

[84] G. E. Athanasiadou, A. R. Nix, and J. P. McGeehan, "A microcellular ray-tracing propagation model and evaluation of its narrow-band and wide-band predictions," *IEEE J. Sel. Areas Commun.*, vol. 18, no. 3, pp. 322–335, Mar. 2000.

[85] A. Schmitz, T. Rick, T. Karolski, L. Kobbelt, and T. Kuhlen, "Beam tracing for multipath propagation in urban environments," in *Proc. 3rd Eur. Conf. Antennas Propag.*, Mar. 2009, pp. 2631–2635.

[86] A. Schmitz, T. Rick, T. Karolski, T. Kuhlen, and L. Kobbelt, "Efficient rasterization for outdoor radio wave propagation," *IEEE Trans. Vis. Comput. Graphics*, vol. 17, no. 2, pp. 159–170, Feb. 2011.

[87] J. Tan, Z. Su, and Y. Long, "A full 3-D GPU-based beam-tracing method for complex indoor environments propagation modeling," *IEEE Trans. Antennas Propag.*, vol. 63, no. 6, pp. 2705–2718, Jun. 2015.

[88] B. R. Epstein and D. L. Rhodes, "GPU-accelerated ray tracing for electromagnetic propagation analysis," in *Proc. IEEE Int. Conf. Wireless Inf. Technol. Syst.*, Aug./Sep. 2010, pp. 1–4.

[89] S. G. Parker *et al.*, "OptiX: A general purpose ray tracing engine," *ACM Trans. Graph.*, vol. 29, no. 4, Jul. 2010, Art. ID 66.

[90] R. Felbecker, L. Raschkowski, W. Keusgen, and M. Peter, "Electromagnetic wave propagation in the millimeter wave band using the NVIDIA OptiX GPU ray tracing engine," in *Proc. 6th Eur. Conf. Antennas Propag.*, Mar. 2011, pp. 488–492.

[91] V. Degli-Eposti, G. Lombardi, C. Passerini, and G. Riva, "Wide-band measurement and ray-tracing simulation of the 1900-MHz indoor propagation channel: Comparison criteria and results," *IEEE Trans. Antennas Propag.*, vol. 49, no. 7, pp. 1101–1110, Jul. 2001.

[92] V. Erceg, S. J. Fortune, J. Ling, A. J. Rustako, and R. A. Valenzuela, "Comparisons of a computer-based propagation prediction tool with experimental data collected in urban microcellular environments," *IEEE J. Sel. Areas Commun.*, vol. 15, no. 4, pp. 677–684, May 1997.

[93] W. C. Y. Lee, "Estimate of local average power of a mobile radio signal," *IEEE Trans. Veh. Technol.*, vol. 34, no. 1, pp. 22–27, Feb. 1985.

[94] R. A. Valenzuela, O. Landron, and D. L. Jacobs, "Estimating local mean signal strength of indoor multipath propagation," *IEEE Trans. Veh. Technol.*, vol. 46, no. 1, pp. 203–212, Feb. 1997.

[95] K. Rizk, J.-F. Wagen, and F. Gardiol, "Influence of database accuracy on two-dimensional ray-tracing-based predictions in urban microcells," *IEEE Trans. Veh. Technol.*, vol. 49, no. 2, pp. 631–642, Mar. 2000.

[96] G. E. Athanasiadou and A. R. Nix, "Investigation into the sensitivity of the power predictions of a microcellular ray tracing propagation model," *IEEE Trans. Veh. Technol.*, vol. 49, no. 4, pp. 1140–1151, Jul. 2000.

[97] Z. Yun, M. F. Iskander, and S. Y. Lim, "The effect of 3D building reconstruction errors on propagation prediction using geospatial data in cyberspace," in *Proc. IEEE AP-S Symp. URSI*, Charleston, SC, USA, Jun. 2009, pp. 1–4.

[98] Z. Yun, S. Y. Lim, and M. F. Iskander, "Use of geospatial resources for radio propagation prediction in urban areas," *IEEE Antennas Wireless Propag. Lett.*, vol. 8, pp. 587–591, 2009.

[99] Z. Yun, M. F. Iskander, S. Y. Lim, D. He, and R. Martinez, "Radio wave propagation prediction based on 3-D building structures extracted from 2-D images," *IEEE Antennas Wireless Propag. Lett.*, vol. 6, pp. 557–559, 2007.

[100] D. He, G. Liang, J. Portilla, and T. Riesgo, "A novel method for radio propagation simulation based on automatic 3D environment reconstruction," in *Proc. 6th Eur. Conf. Antennas Propag.*, Mar. 2012, pp. 1445–1449.

[101] (Feb. 2, 2006). *Shuttle Radar Topography Mission*. [Online]. Available: http://www2.jpl.nasa.gov/srtm

[102] U.S. Geological Survey. (Sep. 2010). *Shuttle Radar Topography Mission*. [Online]. Available: http://srtm.usgs.gov/index.php

[103] (Jan. 2015). *National Elevation Dataset*. [Online]. Available: http://ned.usgs.gov/

[104] Z. Yun, S. Y. Lim, and M. F. Iskander, "Modeling three-dimensional terrain in urban propagation environment using geospatial data in cyberspace," in *Proc. IEEE AP-S Symp. URSI*, Toronto, ON, Canada, Jul. 2010, pp. 1–4.

[105] Z. Yun, N. Omaki, and M. F. Iskander, "Ridge feature extraction and effect on radio propagation for wireless communications," in *Proc. IEEE AP-S Symp. URSI*, Chicago, IL, USA, Jul. 2012, pp. 1–2.

[106] Z. Yun and M. F. Iskander, "Diffraction from multiple ridges: Comparing three- and two-dimensional results," in *Proc. 8th Eur. Conf. Antennas Propag.*, The Hague, The Netherlands, Apr. 2014, pp. 1587–1588.

[107] (Sep. 2013). *The USGS Center for LIDAR Information Coordination and Knowledge*. [Online]. Available: http://lidar.cr.usgs.gov/

[108] S. Haykin, "Cognitive radio: Brain-empowered wireless communications," *IEEE J. Sel. Areas Commun.*, vol. 23, no. 2, pp. 201–220, Feb. 2005.

[109] V. Degli-Esposti, "Ray tracing propagation modelling: Future prospects," in *Proc. 8th Eur. Conf. Antennas Propag.*, The Hague, The Netherlands, Apr. 2014, p. 2232.

ZHENGQING YUN (M'98) received the Ph.D. degree in electrical engineering from Chongqing University, Chongqing, China, in 1994.

He was an Assistant Researcher with the Hawaii Center for Advanced Communications (HCAC) from 2002 to 2005, where he became an Assistant Professor in 2006. He was involved in post-doctoral work with the University of Utah and Southeast University, China, before he joined the University of Hawaii at Manoa (UH), Honolulu, HI. He is currently an Associate Professor with HCAC, College of Engineering, UH.

Dr. Yun's current research interests include radio propagation in complex environments, such as urban, indoor and mountainous areas, and ocean surface and atmospheric ducts. He served as the Technical Program Co-Chair of the IEEE Antenna and Propagation Society International Symposium, Honolulu, in 2007, and the Technical Program Chair of the IEEE International Conference on Wireless Information Technology and Systems, Honolulu, in 2010, and Maui, HI, in 2012. He was an Associate Editor of the IEEE TRANSACTIONS ON VEHICULAR TECHNOLOGY and the IEEE TRANSACTIONS ON ANTENNAS AND PROPAGATION. He is currently an Associate Editor of the IEEE ACCESS.

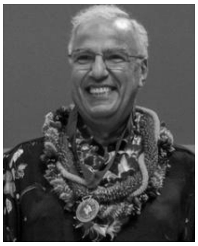

MAGDY F. ISKANDER (F'93) is currently a Professor of Electrical Engineering and the Director of the Hawaii Center for Advanced Communications with the College of Engineering, University of Hawaii at Manoa, Honolulu, HI, USA. He is the Co-Director of the NSF Industry/University Cooperative Research Center with four other universities. He was the 2002 President of the IEEE Antennas and Propagation Society, a Distinguished Lecturer, and the Program Director of the Electrical, Communications, and Cyber Systems Division with the National Science Foundation.

He was a Professor of Electrical and Computer Engineering and the Engineering Clinic Endowed Chair Professor with the University of Utah. He joined the University of Hawaii in 2002. He received many awards for excellence in research and teaching, including the University of Hawaii Board of Regents' Medal for Excellence in Research (2013), the Board of Regents Medal for Teaching Excellence (2010), and the Hi Chang Chai Outstanding Teaching Award (2011 and 2014), which is based on votes by graduating seniors. He also received the IEEE MTT-S Distinguished Educator Award (2013), the IEEE AP-S Chen-To Tai Distinguished Educator Award (2012), and the Richard R. Stoddard Award from the IEEE EMC Society (1992). He was a recipient of the Northrop Grumman Excellence in Teaching Award in 2010, the American Society for Engineering Education (ASEE) Curtis W. McGraw National Research Award in 1985, and the ASEE George Westinghouse National Award for Excellence in Education in 1991. Recently, his students won the first place in the University of Hawaii Business Plan Competition for the CP Stethoscope project. Subsequently, he founded the MiWa Technologies, LLC for medical devices and applications.

He has authored over 250 papers in technical journals, holds nine patents, and has made numerous presentations at national/international conferences. He authored/edited several books, including the textbook entitled *Electromagnetic Fields and Waves* (Prentice Hall, 1992, and Waveland Press, 2001; second edition 2012), and four books in microwave processing of materials published by the Materials Research Society. He is the Founding Editor of the *Computer Applications in Engineering Education* (John Wiley & Sons, 1992–present).

His research in computational and biomedical electromagnetics and wireless communications is funded by the National Science Foundation, the National Institute of Health, the Army Research Office, the U.S. Army CERDEC, the Office of Naval Research, and several corporate sponsors.